

1 Article

## 2 Molecular Evolution in a Peptide-vesicle System

3 Christian Mayer<sup>1\*</sup>, Ulrich Schreiber<sup>2</sup>, María J. Dávila<sup>2</sup>, Oliver J. Schmitz<sup>3</sup>, Amela Bronja<sup>3</sup>, Martin  
4 Meyer<sup>3</sup>, Julia Klein<sup>3</sup>, Sven W. Meckelmann<sup>3</sup>

5 <sup>1</sup>Institute of Physical Chemistry, CENIDE, University of Duisburg-Essen

6 <sup>2</sup>Department of Geology, University of Duisburg-Essen

7 <sup>3</sup>Institute of Applied Analytical Chemistry, University of Duisburg-Essen

8 \* Correspondence: [christian.mayer@uni-due.de](mailto:christian.mayer@uni-due.de), Tel. 0049 201 183 2570

9

10 **Abstract:** Based on a new model of a possible origin of life, we establish an efficient and stable  
11 system undergoing structural reproduction, self-optimization and molecular evolution. This system  
12 is being formed under realistic conditions by the interaction of two cyclic processes, one of which  
13 offering vesicles as the structural environment, the other supplying peptides from a variety of amino  
14 acids as versatile building blocks. We demonstrate that structures growing in a combination of both  
15 cycles have the potential to support their own existence, to undergo chemical and structural  
16 evolution and to develop unpredicted functional properties. The key mechanism is the mutual  
17 stabilization of the peptides by the vesicles and of the vesicles by the peptides together with a  
18 constant production and selection of both. The development of the proposed system over time not  
19 only would represent one of the principles of life, but could also be a model for the formation of  
20 self-evolving structures ultimately leading to the first living cell. The experiment yields clear  
21 evidence on a vesicle-induced accumulation of membrane-interacting peptide which could be  
22 identified by liquid chromatography combined with high-resolution mass spectroscopy. We found  
23 that the selected peptide has an immediate effect on the vesicles, leading to i) reduced vesicle size, ii)  
24 increased vesicle membrane permeability, and iii) improved thermal vesicle stability.

25

26 **Keywords:** Origin of life; evolution; molecular evolution; prebiotic chemistry; peptides; vesicles

27

### 28 1. Introduction

29 It is generally accepted that complex prebiotic structures do not appear accidentally, but instead  
30 form in a long-term process facilitated by random variation, selection and reproduction. This  
31 process, representing a very general form of evolution, must have dominated even the very early  
32 steps leading to very primitive precursors of a living cell. It must have been based on the building  
33 blocks of prebiotic chemistry which potentially have been formed in many different locations on or  
34 near the early Earth [1-9].

35

36 An important fraction of prebiotic compounds are amphiphilic substances, the precursors of  
37 lipids. Their unique tendency to form various mesostructures, most prominently multilayers and

38 vesicles with double-layer membranes, makes them a natural starting point for cell-like  
39 compartments [10-12]. They also have the capability to select and accumulate other prebiotic  
40 molecules [13,14], especially if those molecules are amphiphilic as well [15,16]. Those amphiphilic  
41 mesostructures may occur naturally in a variety of environments, such as shore lines, hot springs  
42 [11,17] or even in bulk liquid phases.

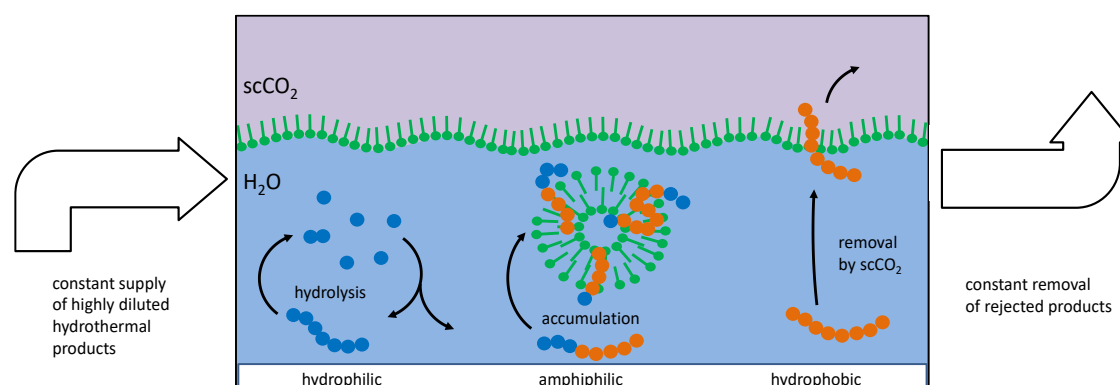
43 A very special environment for the formation of amphiphilic structures are deep-reaching  
44 tectonic fault zones [18]. Recently, we proposed a mechanism of periodic vesicle formation which is  
45 expected to occur in fault zones filled by water and CO<sub>2</sub> [15]. At a depth of approximately -1 km,  
46 pressure and temperature conditions induce a local phase transition between supercritical CO<sub>2</sub>  
47 (scCO<sub>2</sub>) and subcritical gaseous CO<sub>2</sub> (gCO<sub>2</sub>). Various amphiphilic products of hydrothermal  
48 chemistry [19] are expected to accumulate at this point due to the solubility drop in CO<sub>2</sub> and the  
49 presence of large transition-induced interfaces.

50 With additional periodic pressure variations resulting from tidal influences or geyser  
51 phenomena, a cyclic process occurs in which the transition scCO<sub>2</sub> → gCO<sub>2</sub> induces the formation of  
52 water droplets covered by a monolayer of amphiphilic compounds [20]. When migrating through  
53 the interface to the aqueous domain (which by itself is covered by a layer of amphiphiles), the  
54 droplets turn into vesicles with a bilayer membrane [21]. Being thermodynamically unstable, the  
55 vesicles are expected to disintegrate and release their organic contents into the bulk water phase  
56 over time. During the transition gCO<sub>2</sub> → scCO<sub>2</sub>, the organic constituents and the water again become  
57 soluble in the CO<sub>2</sub> phase and the cycle can start again [15]. So, in general, each pressure cycle  
58 corresponds to one generation of vesicles, even though individual vesicles may survive for several  
59 cycles.

60 In the same hydrothermal environment, amino acids are expected to occur [22-24]. Under the  
61 given temperature and pressure conditions and in presence of the water/carbon dioxide interface,  
62 these amino acids undergo spontaneous condensation reactions and form a series of oligopeptides  
63 [16,25]. After a short period of time, the competing processes of condensation and hydrolysis will  
64 lead to an equilibrium situation. In this state, the concentrations of longer oligopeptides are very  
65 small. In a corresponding laboratory experiment, they decrease by approximately one order of  
66 magnitude for each additional amino acid unit [16]. Nevertheless, this process leads to a constant  
67 presence of random oligopeptides of variable length.

68 However, if a given peptide with a specific amino acid sequence is capable of interacting with  
69 the bilayer membranes of the vesicles described above, e.g. by being amphiphilic with an  
70 amphiphilicity profile resembling the one of the membrane, it will integrate into the bilayer struc-  
71 ture. Such an integrated peptide is now protected against hydrolysis and therefore will accumulate  
72 over time. Consequently, its concentration can keep on growing and may surpass the original  
73 equilibrium concentration by several orders of magnitude [16]. At the same time, primarily hydro-  
74 philic peptides are recycled and primarily hydrophobic ones will be eluted by scCO<sub>2</sub> (Figure 1).

75



76

77 Figure.1. Mechanism of peptide selection and accumulation in presence of vesicles. Left: Peptide chains formed  
 78 by hydrophilic amino acids (blue circles) will undergo little interaction with vesicles and remain in the aqueous  
 79 phase where they undergo hydrolysis. Right: Peptide chains formed by hydrophobic amino acids (red circles)  
 80 will eventually be eluted by scCO<sub>2</sub>. Center: Amphiphilic peptides will accumulate in the bilayer membrane and  
 81 remain partially protected against hydrolysis and elution [16].

82 Of course, such an accumulation has consequences for the vesicle structure. If the vesicle is  
 83 being stabilized by the given peptide, its lifetime will increase, maybe even over several pressure  
 84 cycles. This given, the period of protection for the corresponding peptide will also increase, giving  
 85 this peptide further selection advantage over competing peptides. This mutual effect (peptide  
 86 stabilizes the vesicle – the vesicle stabilizes the peptide) has the capability to drive an ongoing  
 87 evolution of a peptide-vesicle system, targeting vesicles with an optimized potential to survive the  
 88 given pressure-cycling conditions. The resulting vesicle system could be the starting point for the  
 89 subsequent development of a living cell [26-28].

90 In the following, we want to report on an experiment which is meant to promote such an  
 91 evolution process. It combines the cyclic formation and destruction of vesicles with the conditions of  
 92 random peptide formation. It involves selection pressure on the vesicle structure and the  
 93 observation of the optimization process over time. Finally, a resulting peptide/vesicle system is  
 94 being studied for its characteristic features regarding vesicle stability and its physical properties.  
 95 Overall, this experiment may be a rare example for a system which develops from a simple towards  
 96 a much more complex one.

97

## 98 2. Materials and Methods

### 99 2.1 Amphiphiles

100 The choice of amphiphiles was driven by two motivations: i) focus on simple chemical  
 101 structures which could easily develop in a hydrothermal system, ii) allow for vesicles which are  
 102 stable at high temperatures, at a broad pH range and in presence of bivalent cations. For the two  
 103 latter conditions, T. Namari and D. Deamer have proposed a mixture of long chain amines with long  
 104 chain fatty acids [29] which are accessible by Fischer-Tropsch chemistry [4]. In order to improve  
 105 temperature stability, C<sub>18</sub> chains have been chosen for both components. Accordingly,  
 106 octadecylamine (GC purity ≥ 99.0%) and octadecanoic acid (GC purity ≥ 94.5%) were purchased  
 107 from Sigma Aldrich.

## 108 2.2 Amino acids

109 The choice of amino acids again followed the condition of being accessible by hydrothermal  
110 chemistry. Initially, only proteinogenic amino acids in their natural L-form were considered for  
111 simplicity. With that, the selection was limited to a set of 12 L-amino acids which were  
112 experimentally accessible under simulated hydrothermal conditions [22]. This includes the  
113 hydrophilic amino acids glycine, serine, threonine, aspartic acid, glutamic acid, and lysine, as well as  
114 the less hydrophilic or hydrophobic varieties alanine, proline, valine, leucine, isoleucine, and  
115 phenylalanine. All amino acids (HPLC or titration purity  $\geq 98.0\%$ ) were purchased from Sigma  
116 Aldrich and were used without further purification.

## 117 2.3 Pressure cell and initial setup

118 In order to simulate conditions given in depths between 1 and 7 km, the high pressure cell (50  
119 mL) of a custom-made phase equilibrium apparatus (SITEC-Sieber Engineering AG, Ebmatingen,  
120 Switzerland) is used as a reaction container. It allows for pressures of up to 1000 bar with manual  
121 fine adjustment, elevated temperatures and constant stirring. It is filled with 25 mL of water  
122 (Millipore Milli-Q water, resistivity 18.2 m $\Omega$ -cm) and 25 mL of carbon dioxide (Air Liquide, GC  
123 purity  $\geq 99.995\%$ ), the latter being either in the gaseous or in the supercritical state depending on the  
124 pressure and temperature conditions. A system of valves and pressure regulations allows one to add  
125 or to remove samples from both phases without changing the pressure inside the cell. All  
126 amphiphiles and amino acids were added to the aqueous phase prior to the start of the experiment.  
127 The concentrations of the amphiphiles octadecylamine and octadecanoic acid were adjusted to 0.01  
128 M each, all 12 amino acids were added in 0.067 M concentration in the aqueous solution.

## 129 2.4 Evolution experiment

130 In order to accelerate the peptide formation cycle and to induce selection pressure on the  
131 vesicles, the temperature inside the cell is kept at 120°C during the whole experiment. The pressure  
132 is repeatedly switched between 100 bar and 70 bar on a regular time scale (every 30 min). During  
133 each pressure cycle, a phase transition from supercritical scCO<sub>2</sub> to gaseous gCO<sub>2</sub> and vice versa is  
134 induced. In each cycle, the transition towards gCO<sub>2</sub> is accompanied by the appearance of  
135 micrometer-sized droplets which, in contact with the bulk aqueous phase, form vesicles (see [15] for  
136 micrographs). On the other hand, the transition towards scCO<sub>2</sub> leads to a depletion of amphiphiles  
137 in the aqueous phase and therefore to (at least partial) vesicle disintegration. Cyclic pressure changes  
138 are induced by a counterbalance piston directly connected to the cell. The total evolution experiment  
139 is run for 160 h and involves 85 pressure cycles. Samples of the aqueous phase (300  $\mu$ L) are taken at  
140  $t=0$ ,  $t=16$  h,  $t=44$  h,  $t=90$  h, and  $t=160$  h. Due to the presence of CO<sub>2</sub> at high pressure, the aqueous  
141 solution is quite acidic with a pH around 3.

## 142 2.5 PFG-NMR experiments

143 The PFG-NMR experiments basically follow a scheme which has been applied in earlier studies  
144 on vesicle dispersions [30, 31]. All corresponding <sup>1</sup>H diffusion experiments are run on a 500 MHz

145 DRX spectrometer (Bruker BioSpin GmbH, Rheinstetten, Germany) with a Bruker DIFF30 probe  
146 head (1200 G/cm maximum field gradient). All measurements were performed at 298 K in a 5 mm  
147 Shigemi NMR sample tube adding 10% D<sub>2</sub>O for spin locking. As a pulse program, the stimulated  
148 echo pulse sequence is combined with two gradient pulses. A total number of 16 scans is used for  
149 each measurement. The spacing  $\Delta$  between the two gradient pulses is set to 25, 50 and 100 ms. The  
150 gradients are adjusted to strengths G between 1.5 G/cm and 750 G/cm, the gradient pulse duration  $\delta$   
151 is set to 2.0 ms. All resulting echo intensities are plotted logarithmically against the parameter  
152  $\gamma^2 G^2 \delta^2 (\Delta - \delta/3)$  with  $\gamma$  being the gyromagnetic ratio of the hydrogen (<sup>1</sup>H) nucleus. In these so-called  
153 Stejskal-Tanner-plots, each slope corresponds to the negative diffusion coefficient of the observed  
154 system component.

155 In order to observe the development of the vesicle properties over time, the experiments are  
156 repeated over extended time periods. In order to study the effect of the peptide, all measurements  
157 are compared with results on original vesicles. The thermal stability of the vesicles with and without  
158 peptides is assessed by introducing storage intervals at elevated temperature between the  
159 measurements (T= 50°C).

## 160 2.6 Identification of accumulated peptides

161 Each sample (300  $\mu$ L, see section 2.4) was centrifuged in order to separate dispersed solid  
162 products from the aqueous solution, basically consisting of vesicles. The separated solid products  
163 were quantified and dissolved in 150  $\mu$ L isopropanol. Prior to analysis, these samples were diluted  
164 1:1 (v/v) with HPLC-water and analyzed along with blank samples (isopropanol/water; 1:1; v/v) for  
165 background subtraction. Both the sample and the blank were analyzed three times. Global peptide  
166 analysis was performed on an Agilent 1290 Infinity liquid-chromatography system consisting of a  
167 1290 Infinity binary pump (G4220A) with a Jet Weaver V35 mixer, a 1290 Infinity HiP sampler  
168 (G4226A), a 1290 Infinity Thermostated Column compartment (G1316C) coupled to an IM-qTOF-MS  
169 (Agilent 6560). Separation was performed on a C18 reversed phase column (Aeris Peptide XB-C18;  
170 150 x 2.1 mm; 1.7  $\mu$ m; Phenomenex Aschaffenburg, Germany) using water and 0.1% formic acid as  
171 eluent A and acetonitrile acidified with 0.1% formic acid as eluent B. The gradient started at 5% B for  
172 2 min, linear to 85% B after 20 min, linear to 95% B after 25 min and hold 95% B for 10 min. The  
173 column was re-equilibrated at the initial conditions for 10 min. The total run time was 45 min at a  
174 flow rate of 0.1 mL/min, the injection volume amounted to 10  $\mu$ L. The column was kept at room  
175 temperature. LC flow was introduced into the IM-qTOF-MS using a dual Agilent Jet Stream  
176 Electrospray Ionization (AJS ESI) source operating in the positive mode. Source parameters were as  
177 follows: capillary 5000 V, nozzle voltage 500 V, nebulizer gas 20 psi, sheath gas 12 L/min (both N<sub>2</sub>),  
178 dry gas temperature was set to 200 °C and sheath gas temperature to 325 °C. Spectra were recorded  
179 in q-TOF only mode between m/z 50-3200.

180 For molecular feature finding, the MassHunter Qualitative Analysis (B.07.00) was used. Background  
181 ions from blank analysis were removed from the resulting feature list using Mass Profiler  
182 Professional (12.6.1) to avoid false positive results. Subsequently, feature list was searched for  
183 possible peptides using an in-house software tool.

184 MS<sup>n</sup> analysis of possible peptides was carried out on a Merck-Hitachi D-7000 HPLC system  
185 equipped with an L-7100 quaternary pump and an L-7200 autosampler coupled to a Bruker Amazon  
186 Speed iontrap MS (Bruker Daltonics, Bremen, Germany). LC conditions were the same as described  
187 above except the flow rate of the mobile phase, which was changed to 0.15 mL/min. ESI parameters  
188 were as follows: capillary 5000 V, end plate offset 500 V, nebulizer gas 20 psi, dry gas 3 L/min (both  
189 N<sub>2</sub>) and dry gas temperature was set to 200 °C. The MS<sup>n</sup> experiment was carried out by selecting the  
190 precursor ion of m/z 864.5 and scanning the resulting fragment ions from m/z 200 to 875 after  
191 activation with an amplitude of 1.0.

## 192 **2.7 Peptide synthesis and vesicle reconstruction**

193 The peptide NH<sub>2</sub>-Lys-Ser-Pro-Phe-Pro-Phe-Ala-Ala-OH (being the largest of the accumulated  
194 species) was synthesized commercially by APeptide Co., Ltd (Shanghai, China). The total amount of  
195 7 mg was used in portions to reassemble the vesicle structure which has led to its accumulation. In  
196 each experiment, 2.6 mg of the peptide were added to 100 μL of a vesicle dispersion formed by a 1:1  
197 mixture of 20 millimolar solutions of octadecanoic acid and octadecylamine at pH=3 (adjusted with  
198 1N HCl) after 6 cyclic pressure cycles in the high pressure cell. Subsequently, the resulting vesicle  
199 dispersion was submitted to field gradient NMR experiments in order to study their average size,  
200 membrane properties and thermal stability.

201

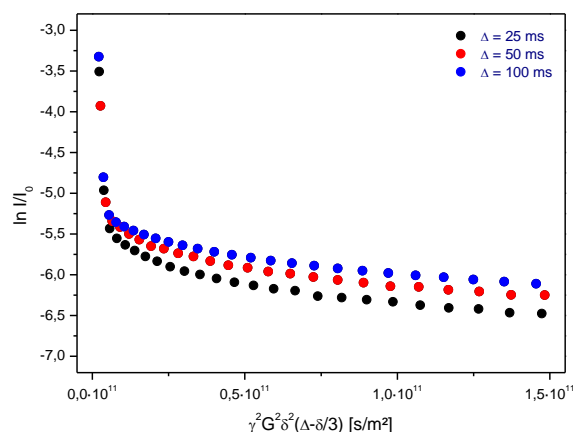
## 202 **3 Results**

### 203 **3.1 Vesicle formation**

204 Experimental evidence for the vesicle formation during the pressure cycling is gained from  
205 optical microscopy and PFG-NMR [15,16]. The volume-averaged diameter of the vesicles amounts to  
206 600 nm under the given circumstances, but generally depends on the rate of decompression. Some of  
207 the vesicles obviously show multilamellar structure and contain internal vesicles, both features  
208 possibly deriving from the fusion of droplets in the gas phase [15,16]. The vesicle structure formed  
209 by bilayers of amphiphilic molecules is further supported by PFG-NMR measurements which show  
210 the presence of encapsulated water molecules inside membranes of relatively low permeability  
211 (Figure 2).

212





213

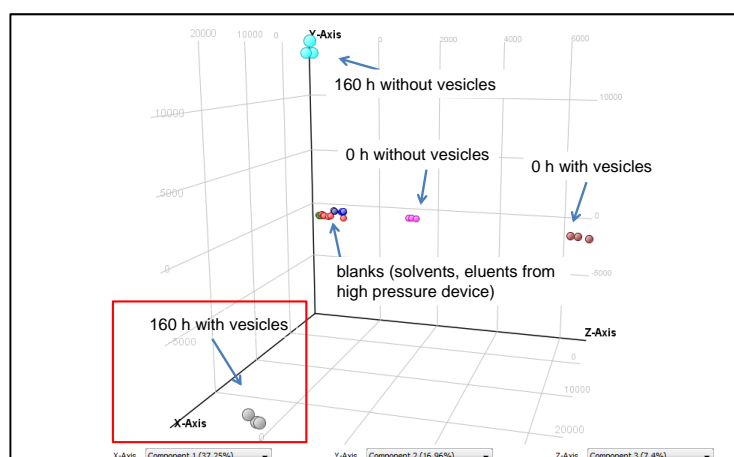
214 Figure 2. Stejskal-Tanner-plot of PFG-NMR data obtained on water molecules in a sample of the aqueous phase during an  
 215 evolution experiment. The steep initial part of the echo decay corresponds to free water, the following shallow part to  
 216 encapsulated water inside the vesicles. The values for  $\Delta$  (25, 50 and 100 ms) refer to the spacing between the gradient pulses.

217

218 In this set of plots, the initial, very steep decay marks the free water molecules, the negative  
 219 slope corresponds to the self-diffusion coefficient of bulk water. The shallow part of each plot refers  
 220 to those water molecules which are encapsulated inside the vesicles. The negative slope of this part  
 221 is in accordance with a self-diffusion coefficient deriving from the Brownian motion of the vesicles.  
 222 On average, it amounts to  $7.1 \cdot 10^{-13} \text{ m}^2/\text{s}$  which, assuming the viscosity of water, corresponds to a  
 223 vesicle diameter of approximately 600 nm. The PFG-NMR data obtained on the samples from the  
 224 aqueous phase document the presence of vesicles over the full duration of the evolution experiment.  
 225 Within its given period of 160 h, the diffusion constant as well as the vesicle diameter show a  
 226 random variability of  $\pm 10\%$ .

### 227 3.2 Peptide formation

228 During the same course of regular sampling, the peptides are followed by two-dimensional  
 229 liquid chromatography and mass spectrometry. A principal component analysis (Figure 3) on  
 230 samples taken after 0 h and 160 h reveals the presence of a fraction of molecules which i) is not  
 231 present at the beginning of the experiment ( $t = 0 \text{ h}$ ), ii) is not present in absence of vesicles, and iii) is  
 232 not present in raw materials (solvents, eluents). Consequently, this fraction of molecules (red frame  
 233 in Fig. 3) only forms in presence of vesicles and over time and therefore should contain all species  
 234 which accumulated during the evolution process.



235

236 Figure 3. Principal component analysis on samples from an evolution experiment taken after 0 and 160 h. The red box  
 237 labels the entity of molecules which are absent at  $t = 0$  h and only form in presence of vesicles over time.

238 All samples taken during the experiment are carefully analyzed for oligopeptides formed by the  
 239 12 amino acids listed in section 2.2. The analyses not only reveal the amino acid composition, but  
 240 also allow for a rough estimation of the peptide concentrations. Selecting the species with the  
 241 steepest concentration increase over time, the following oligopeptides, all belonging to the fraction  
 242 “160 h with vesicles” (Figure 3), have been identified:

243 Thr Thr Pro

244 Lys Pro Pro Phe

245 Lys Lys Gly Pro Ala

246 Lys Ser Pro Ala Phe

247 Lys Pro Gly Gly Gly Phe

248 Lys Ser Pro Pro Ala Ala Phe Phe

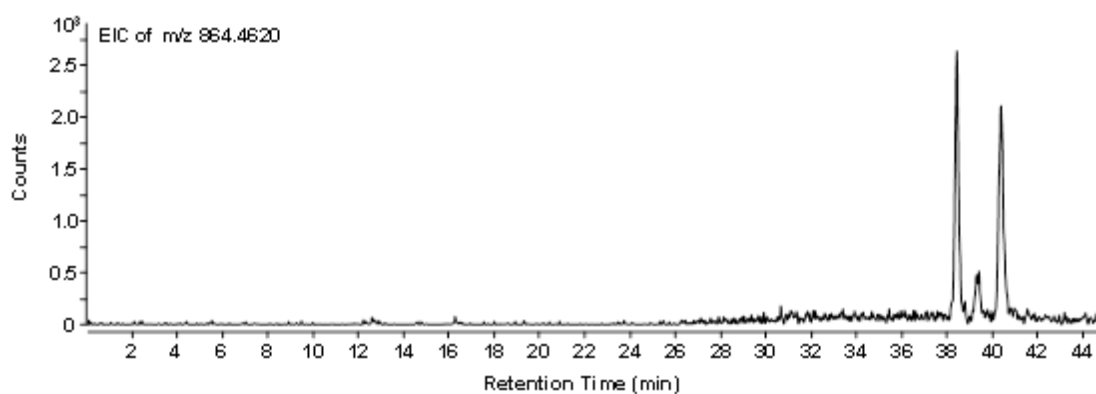
249 The compositions given above do not represent the actual sequence of the amino acids. Instead,  
 250 the amino acids are listed according to their polarity (most polar ones first). As a striking feature, the  
 251 amino acid lysine occurs in almost all of the peptides. This may be related to its possible function as  
 252 a charged head group: offering a free amino residue, it is expected to be almost quantitatively  
 253 protonated in the given acidic environment (see section 2.4) and therefore will carry at least one  
 254 positive charge. Another interesting property of the longer peptides is the abundance of  
 255 hydrophobic amino acids. With 60-80% occurrence, they form the largest section of the peptide  
 256 chains. Most peptides also contain phenylalanine, which is the most hydrophobic amino acid within  
 257 the given selection. Altogether, one can postulate that all given peptides at least have the potential to  
 258 be strong amphiphiles.



259 Regarding its potential to integrate into vesicle membranes and to take influence on the vesicle  
260 properties, the last species (Lys Ser Pro Pro Ala Ala Phe Phe) appears to be the most promising  
261 candidate. Therefore, this octapeptide was submitted to a closer analysis of its amino acid sequence  
262 using MS<sup>n</sup> analysis with an iontrap-MS. Due to the low concentration of the peptide, the  
263 identification of the sequence was complicated and included some plausible considerations.  
264 According to the resulting data, the charged lysine residue occurs at the amino-terminated end of  
265 the peptide chain, most likely followed by the serine. At the carboxylic end of the chain, we most  
266 probably deal with a set of two alanine segments. That leaves two phenylalanine and two proline  
267 residues for the inner part of the chain. Due to the relatively bulky phenyl side group, it is less likely  
268 that two phenylalanine units are directly connected. Proline, on the other hand, induces a relatively  
269 stiff chain conformation and has the property to induce turns in the peptide chain. Therefore, two  
270 prolines are unlikely to be directly connected as well. That leaves an inner sequence of either Pro Phe  
271 Pro Phe or Phe Pro Phe Pro for the central part of the octapeptide. Based on these findings and  
272 conclusions, we decided for

273  $\text{NH}_2\text{-Lys-Ser-Pro-Phe-Pro-Phe-Ala-Ala-OH}$

274 as the most likely structure of the given peptide. In the individual chromatogram of the peptide  
275 (Figure 4), three peaks can be observed which represent the same composition of the peptide, but  
276 obviously different sequences. All three peptides have accumulated in the evolution experiment.  
277 Therefore, we can conclude that there is a certain variability in the sequence and that the sequence  
278 given above is most likely among those accumulated species.



279

280 Figure 4: Extracted ion chromatogram of the selected mass peak representing the octapeptide composition  
281  $\text{NH}_2\text{-Lys-Ser-Pro-Phe-Pro-Phe-Ala-Ala-OH}$  ( $m/z = 863.4548$  g/mol for the non-protonated species). The three  
282 signals (two strong and one weak) presumably correspond to different amino acid sequences with the same  
283 overall composition.

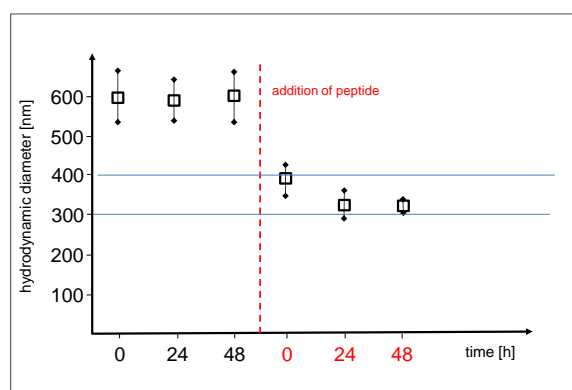
284

### 285 3.3 Vesicle reassembly

286 Having identified an accumulated species, the main purpose of this study is to elucidate why  
287 this particular octapeptide had the potential to be selected during the evolution experiment. This

288 question is efficiently approached by a study on the special properties of a corresponding  
289 peptide-vesicle system. Since the concentration of the octapeptide in the overall mixture is still  
290 extremely low, this task has to be performed on a reconstituted system. For this purpose, the  
291 octapeptide NH<sub>2</sub>-Lys-Ser-Pro-Phe-Pro-Phe-Ala-Ala-OH is commercially synthesized and added to a  
292 neat vesicle dispersion which has been prepared in the high pressure cell. The resulting  
293 peptide-vesicle system is carefully studied and compared to the original vesicle system.

294 When added to the original vesicles, the peptide has an immediate influence on the vesicle size  
295 (Figure 5). The volume-averaged hydrodynamic radius of the vesicles is determined from the slope  
296 of the shallow part of the Stejskal-Tanner plots. This slope corresponds to the negative diffusion  
297 coefficient associated to the Brownian motion, which in turn allows for the calculation of the vesicle  
298 size at a given temperature and solvent viscosity. From an average value of 600 nm, the diameter is  
299 suddenly reduced to 300-400 nm by the action of the peptide. Before and after the addition of the  
300 peptide, the diameter is relatively stable over time.



301

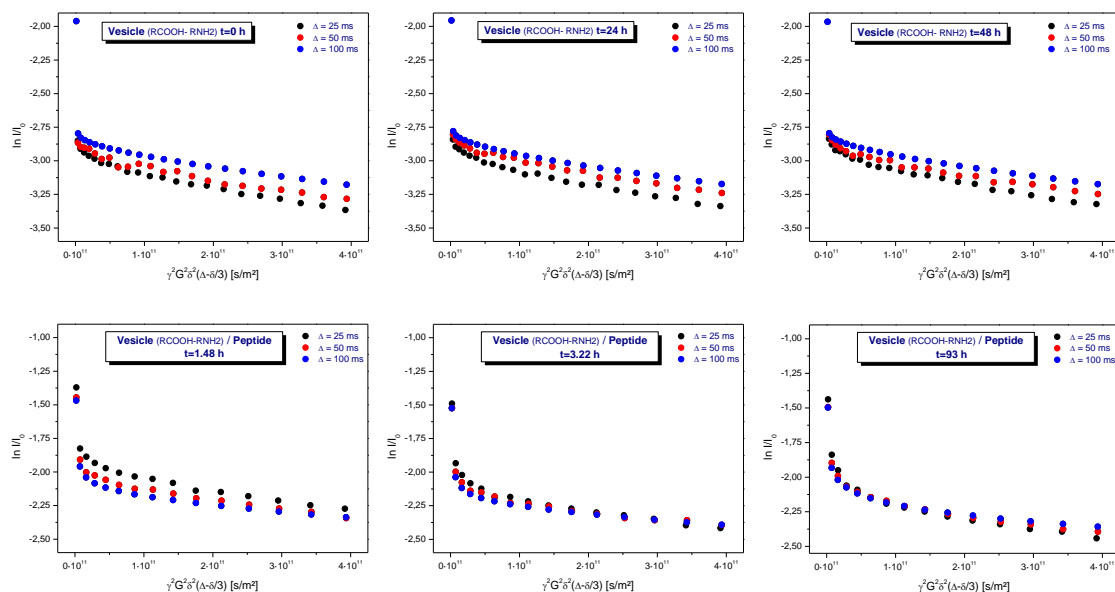
302 Figure 5: Average diameter of the vesicles before (left) and after the addition of the peptide  
303 NH<sub>2</sub>-Lys-Ser-Pro-Phe-Pro-Phe-Ala-Ala-OH (right of dotted line). The error bars mark the experimental  
304 variability.

305

306 A special feature of the PFG-NMR measurement and of the resulting Stejskal-Tanner plot is its  
307 sensitivity for the permeation process. The variation of the level of the shallow part with the gradient  
308 pulse spacing  $\Delta$  allows for direct conclusions on the membrane permeability for the observed  
309 molecules (water in the given case). Due to the exchange-related loss of encapsulated water  
310 molecules over time, the permeation process leads to a corresponding drop of the final level of the  
311 plot with increasing pulse spacing  $\Delta$ . In case of the neat vesicles, this drop is not observable. Instead,  
312 there is even an inverted sequence (the level for 100 ms is higher than the one for 25 ms), which  
313 results from internal water diffusion inside of the vesicle volume (Figure 6, top row). However, as  
314 soon as the peptide is added, the sequence changes drastically. Actually, the sequence now is typical  
315 for a rapid permeation process: the level for 25 ms is higher than the one for 100 ms (Figure 6, first  
316 image in the bottom row). Obviously, there is a significant loss of encapsulated water molecules in  
317 the time interval between 25 and 100 ms which is induced by the addition of the peptide.

318

319



320

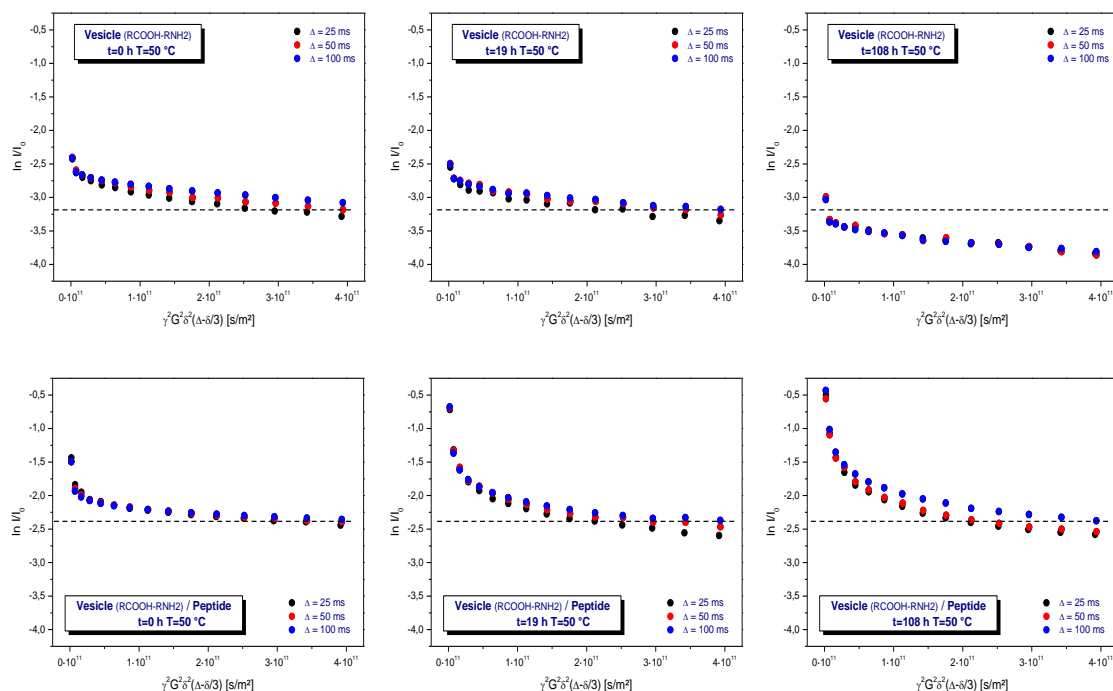
321 Figure 6: Steijskal-Tanner plots determined on water for neat vesicles (top row) and after the addition of the  
 322 peptide NH<sub>2</sub>-Lys-Ser-Pro-Phe-Pro-Phe-Ala-Ala-OH (bottom row). As determined from the inversion of the  
 323 sequence for  $\Delta = 25, 50$  and  $100$  ms, the peptide causes a temporary increase of the vesicle membrane  
 324 permeability for water (bottom row, left). Within several hours, the sequence slowly returns to the original one,  
 325 indicating the loss of the original permeability over time (bottom row, from left to right).

326 However, this situation changes over time. Within 1.5 h, the permeation-induced drop collapses,  
 327 and gradually returns to the original one observed on neat vesicles (Figure 6, bottom row, left to  
 328 right). Finally, after 108 h storage at elevated temperature (50°C), the original sequence is reached  
 329 (Figure 7, bottom row, right).

330 The most interesting aspect of the peptide selection is the potential influence on the thermal  
 331 stability of the vesicles. For the assessment of the given peptide, the PFG-NMR measurements have  
 332 been repeated during a period of high-temperature storage (50°C, 100h), for neat vesicles as well as  
 333 for the peptide-vesicle system. The result is shown in Figure 7. It reveals a significant thermal  
 334 instability of the neat vesicles, as determined from the drop of the final plateau values (Figure 7, top  
 335 row). The loss of the encapsulated fraction corresponds to a half-life time around 100 h. In contrast,  
 336 no such loss is observed for vesicle dispersions after the addition of the peptide (Figure 7, bottom  
 337 row). This demonstrates a strong stabilizing effect on the vesicles which is induced by the selected  
 338 octapeptide NH<sub>2</sub>-Lys-Ser-Pro-Phe-Pro-Phe-Ala-Ala-OH.

339

340



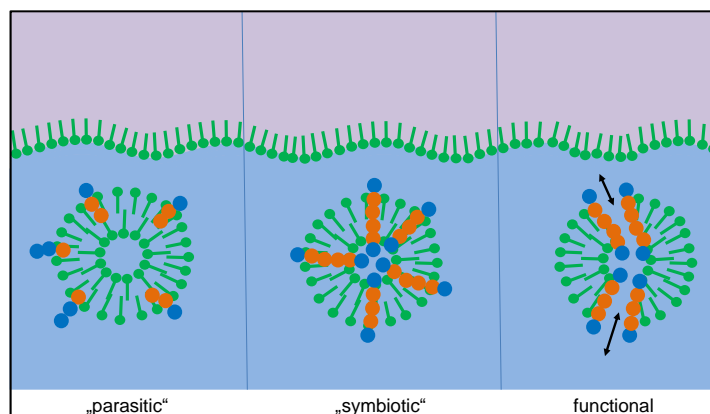
341

342 Figure 7: Steijskal-Tanner plots determined on water for neat vesicles (top row) and after the addition of the  
 343 peptide NH<sub>2</sub>-Lys-Ser-Pro-Phe-Pro-Phe-Ala-Ala-OH (bottom row). Both series correspond to storage at 50°C for  
 344 0, 19 and 100 h. As determined from the shift of the final plot level, there is a significant decomposition of the  
 345 neat vesicles (top row). No such decomposition is observed on vesicles containing the peptide, revealing its  
 346 stabilizing effect.

347

#### 348 4 Discussion

349 The experimental results clearly show a significant fraction of peptides which i) are not yet  
 350 present at the beginning of the experiment and gradually form over time, and ii) only form in  
 351 presence of the vesicles. Among these, a few peptides are sticking out in terms of their concentration  
 352 increase over time, most prominently the octapeptide NH<sub>2</sub>-Lys-Ser-Pro-Phe-Pro-Phe-Ala-Ala-OH.  
 353 Obviously, this peptide has been accumulated in a selection process induced by the presence of  
 354 membrane vesicles. Looking at possible mechanisms of peptide selection in detail, one can  
 355 differentiate between three possible criteria favoring different types of amphiphilic peptides (Figure  
 356 8) [16]. In the following, we briefly describe the three selection criteria and discuss the possible  
 357 contribution of the selected peptide NH<sub>2</sub>-Lys-Ser-Pro-Phe-Pro-Phe-Ala-Ala-OH:  
 358



359

360

361

362

363

364

365

366

367

368

369

370

371

372

373

374

375

376

377

378

379

380

381

382

383

384

385

386

387

388

389

390

391

Figure 8. Possible targets of a selection process of peptide-vesicle systems. Integration and protection of peptide (parasitic), additional thermal stabilization of the vesicle structure (symbiotic), and introduction of a peptide-induced function (functional).

**1) Integration.** Amphiphilic peptides with an amphiphilicity profile reflecting the one of the bilayer integrate into the vesicle membrane. Hereby, they gain an individual selection advantage as they are partially protected against hydrolysis and as they become less easily eluted from the vesicle zone. For this selection criterion, the effect of the peptide on the stability of the vesicle is irrelevant, hence one could call this mechanism a parasitic one.

The amphiphilicity profile of the selected peptide  $\text{NH}_2\text{-Lys-Ser-Pro-Phe-Pro-Phe-Ala-Ala-OH}$  is clearly predestinated by its sequence. In the given acidic environment ( $\text{pH}=3$ ), the initial lysine group, offering an additional amino residue, will carry at least one positive charge, possibly even two since it forms the amino end of the chain. Serine is quite hydrophilic as well and can therefore contribute to the polar head of the molecule. The residual chain of the peptide is being formed by six non-polar amino acids (pairs of proline, phenylalanine, and alanine) with a clear potential to represent the hydrophobic part of the molecule. Altogether, the selected octapeptide can be regarded as strongly amphiphilic. All experimental results support its expected rapid membrane integration. The changes of the vesicle size (Figure 5) and vesicle membrane permeability (Figure 6) occur almost instantaneously and can only be interpreted by an intense and integrative peptide-membrane interaction.

**2) Stabilization.** In this “symbiotic” interaction, amphiphilic peptides are again being protected by vesicles, but in turn they also stabilize the vesicle structure. This leads to a mutual advantage connected to the formation of the peptide-vesicle system. With increased stability, the vesicles could even survive several pressure cycles (“generations”), therefore giving the peptide an increased degree of protection over a longer period of time. Consequently, this “symbiotic” effect would lead to an even stronger selection advantage of the peptide.

In the given experiment, the selected peptide  $\text{NH}_2\text{-Lys-Ser-Pro-Phe-Pro-Phe-Ala-Ala-OH}$  clearly has a protective effect on the vesicles. While the original vesicles show a significant thermal decomposition over 100 h at  $50^\circ\text{C}$  (Figure 7, top row), the peptide-vesicle system seems to be stable under the same conditions (Figure 7, bottom row). Even though there is no plausible interpretation of the mechanism, the effect of thermal stabilization is obvious. An additional factor for the stability-related selection of vesicles may be the vesicle size. During the decompression step of the

392 pressure cycling, CO<sub>2</sub> bubbles are generated which have the potential to disrupt vesicles if they form  
393 inside their inner volume. Consequently, smaller vesicles have better chances to stay intact, giving  
394 peptides which reduce the vesicle size a selection advantage. This may explain the effect of the  
395 selected peptide on the vesicle diameter (Figure 5).

396 **3) Function.** The selection of peptides could go even beyond the effect of simple mechanical  
397 stabilization and lead to more complex ("functional") survival mechanisms. A possible example may  
398 be a membrane structure which allows for the increased permeation of solvent through the  
399 membrane (like, e.g., by the formation of a channel structure [32]). In the vesicle cycle, the vesicles  
400 are generated with a natural ionic concentration gradient across the membrane which destabilizes  
401 their structure by the resulting osmotic stress. Permeation through the membrane could cause a  
402 rapid relaxation of this gradient, leading to a longer vesicle lifetime and resulting in a corresponding  
403 selection advantage for the permeation-inducing peptide.

404 Obviously, the selected peptide NH<sub>2</sub>-Lys-Ser-Pro-Phe-Pro-Phe-Ala-Ala-OH causes an increased  
405 degree of water permeation through the vesicle membranes (Figure 6), at least for a limited period of  
406 time. This period, however, is sufficient for an equilibration of concentration gradients which mainly  
407 consist in the dissolved amino acids (their overall concentration being 0.8 M in the outer aqueous  
408 phase, but nearly zero in the inner phase of the vesicles). Again, there is no clear interpretation of the  
409 mechanism and the reason why it only acts temporarily, but the effect of water permeation is  
410 significant and will probably include dissolved components as well. It will lead to a rapid decrease  
411 of the osmotic pressure and therefore increase the survival rate of the vesicles.

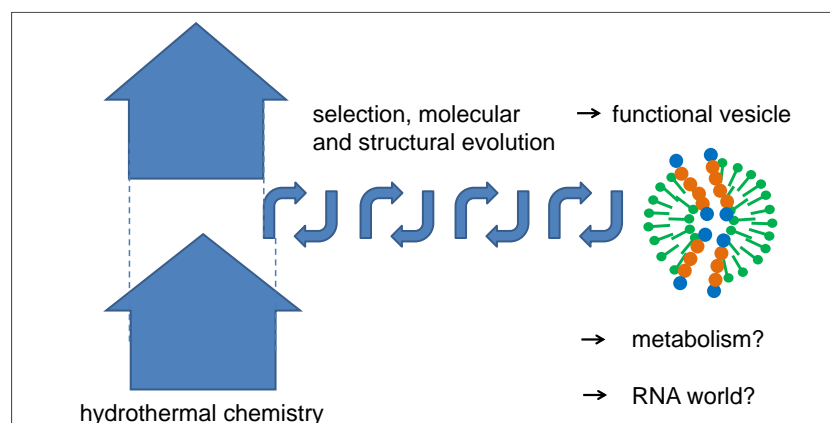
412

## 413 **5 Conclusion**

414 The peptide NH<sub>2</sub>-Lys-Ser-Pro-Phe-Pro-Phe-Ala-Ala-OH selected in the described experiment  
415 may be an example for the result of a molecular evolution process occurring under very primitive  
416 and quite natural conditions. With the given sequence, it obviously integrates into the vesicle  
417 membrane, increases its thermal stability as well as its permeability and decreases the vesicle size.  
418 All these effects can be interpreted as suitable survival strategies of the peptide-vesicle system  
419 leading to prolonged lifetimes under the given circumstances.

420 Even though the described mechanism of peptide selection misses the capability for identical  
421 reproduction, the mechanism of selection from a large pool of random peptides over a long period of  
422 time can be quite efficient. Both conditions are definitely fulfilled for peptides in hydrothermal  
423 sources. The entropic driving force of the process consists in the expansion and dilution of a large  
424 amount of hydrothermal products rising in the Earth's crust, from which a small fraction is selected  
425 over a long and iterative process (Figure 9). The outcome may be a peptide-vesicle system which has  
426 developed a set of functions leading to its long-term survival. In the evolution process on early  
427 Earth, this may have included an early stage of a primitive metabolism which could have taken  
428 advantage of concentration gradients as an initial energy source by the use of catalytically active  
429 peptide channels. Finally, such a functional peptide-vesicle system could also have formed an ideal  
430 platform for a subsequent RNA world.

431



432

433

Figure 9. Schematic diagram of a possible structural evolution of vesicles by repeated optimization steps in tectonic fault zones.

434

435

436

437

## References

438

1 Dyson, F.J. *Origins of Life*, Cambridge University Press, Cambridge 1999.

439

2 Trainer, M.G. Atmospheric prebiotic chemistry and organic hazes. *Curr Org Chem* **2013**, *17*, 1710-1723.

440

441

3 Airapetian, V.S., Glocer, A., Gronoff, G., Hébrard, E., Danchi, W. Prebiotic chemistry and atmospheric warming of early Earth by an active young sun. *Nat Geosci* **2016**, *9*, 452-455.

442

443

4 Simoneit, B.R.T. Prebiotic organic synthesis under hydrothermal conditions: an overview. *Adv Space Res* **2004**, *33*, 88-94.

444

445

5 Matsuno, K. Hydrothermal reaction. In: *Encyclopedia of Astrobiology* (Springer, Berlin) **2011**, 788-790

446

6 Lawless, J.G. Amino acids in the Murchison meteorite. *Geochim Cosmochim Acta* **1973**, *37*, 2207-2212.

447

448

7 Guillemin, J.C., Bouyahyi, M., Riague, E.H. Prebiotic, planetary and interstellar chemistry starting from compounds detected in the interstellar medium. *Adv Space Res* **2004** *33*, 81-87.

449

450

8 Martins, Z., Botta, O., Fogel, M.L., Sephton, M.A., Glavin, D.P., Watson, J.S., Dworkin, J.P., Schwartz, A.W., Ehrenfreund, P. Extraterrestrial nucleobases in the Murchison meteorite. *Earth Planet Sci Lett* **2008**, *270*, 130-136.

451

452

9 Schreiber, U., Mayer, C., Schmitz, O.J., Rosendahl, P., Bronja, A., Greule, M., Keppler, F., Mulder, I., Sattler, T., Schöler, H.F. Organic compounds in fluid inclusions of Archean quartz – analogues of prebiotic chemistry on early Earth. *PLoS ONE* **2017**, *12*(6), e0177570.

453

454

10 Deamer, D., Dworkin, J.P., Sandford, S.A., Bernstein, M.P., Allamandola, L.J. The first cell membranes. *Astrobiology* **2002**, *2*(4), 371-381.

455

456

11 Deamer, D. The role of lipid membranes in life's origin. *Life* **2017**, *7*(1), 5.

457

458

12 Sakuma, Y., Imai, M. From vesicles to protocells: The roles of amphiphilic molecules. *Life* **2015**, *5*(1), 651-675.

459

460

13 Black, R.A., Blosser, M.C. A self-assembled aggregate composed of a fatty acid membrane and the building blocks of biological polymers provides a first step in the emergence of protocells. *Life* **2016**, *6*, 33.

461

462



- 463 14 Black, R.A., Blosser, M.C., Stottrup, B.L., Tavakley, R., Deamer, D.W., Keller, S.L. Nucleobases bind to  
464 and stabilize aggregates of a prebiotic amphiphile, providing a viable mechanism for the emergence  
465 of protocells. *PNAS* **2013**, *110*, 13272-13276.
- 466 15 Mayer C., Schreiber, U., Dávila, M.J. Periodic vesicle formation in tectonic fault zones – an ideal  
467 scenario for molecular evolution. *Orig Life Evol Biosphere* **2015**, *45*, 139-148.
- 468 16 Mayer, C., Schreiber, U., Dávila, M.J. Selection of prebiotic molecules in amphiphilic environments.  
469 *Life* **2017**, *7*, 3.
- 470 17 Damer, B., Deamer, D., Coupled phases and combinatorial selection in fluctuating hydrothermal  
471 pools: a scenario to guide experimental approaches to the origin of cellular life. *Life* **2015**, *5*, 872-887.
- 472 18 Schreiber, U., Locker-Grütjen, O., Mayer, C. Hypothesis: Origin of life in deep-reaching tectonic faults.  
473 *Orig Life Evol Biosph* **2012**, *42*, 47-54.
- 474 19 Rushdie, A.I., Simoneit, B.R. Abiotic condensation synthesis of glyceride lipids and wax esters under  
475 simulated hydrothermal conditions. *Orig Life Evol Biosph* **2006**, *36*, 93-108.
- 476 20 Tuck, A. The role of atmospheric aerosols in the origin of life. *Surv Geophys* **2002**, *23*, 379-409.
- 477 21 Dobson, C.M., Allison, B.G., Tuck, A.F., Vaida, V. Atmospheric aerosols as prebiotic chemical  
478 reactors. *PNAS* **2000**, *97*, 11864-11868.
- 479 22 Marshall, W.L. Hydrothermal synthesis of amino acids. *Geochim Cosmochim Acta* **1994**, *58*,  
480 2099-2106.
- 481 23 Andersson, E.M., Holm, N.G. The stability of some selected amino acids under attempted redox  
482 constrained hydrothermal conditions. *Orig Life Evol Biosphere* **2000**, *30*, 9-23.
- 483 24 Kitadai, N. Energetics of amino acid synthesis in alkaline hydrothermal environments. *Orig Life Evol*  
484 *Biosphere* **2015**, *45*, 377-409.
- 485 25 Lemke, K.H., Rosenbauer, R.J., Bird, D.K. Peptide synthesis in early Earth hydrothermal systems.  
486 *Astrobiology* **2009**, *9*, 141-146.
- 487 26 Deamer, D.W. The first living systems: a bioenergetics perspective. *Microbiol Mol Biol Rev* **1997**, *61*,  
488 239-261.
- 489 27 Segré, D., Ben-Eli, D., Deamer, D.W., Lancet, D. The lipid world. *Orig Life Evol Biosph* **2001**, *31*,  
490 119-145.
- 491 28 Chen, I.A., Walde, P. From self-assembled vesicles to protocells. *Cold Spring Harb Perspect Biol*  
492 **2010**, *2*:a002170.
- 493 29 Namari, T., Deamer, D.W. Stability of model membranes in extreme environments. *Orig Life Evol*  
494 *Biosph* **2008**, *38*(4), 329-341.
- 495 30 Mayer, C., Bauer, A. Molecular exchange through capsule membranes observed by pulsed field  
496 gradient NMR. *Prog Coll Polym Sci* **2006**, *133*, 22-29.
- 497 31 Bauer, A., Hauschild, S., Stolzenburg, M., Förster, S., Mayer, C., Molecular exchange through  
498 membranes of P2V-PEO vesicles, *Chem Phys Lett* **2006**, *419*, 430-433.
- 499 32 Futaki, S. Peptide ion channels: design and creation of function. *Peptide Sci* **1998**, *47*, 75-81.
- 500